Influence of the Oxygen Concentration on the Formation of Crystalline Phases of TiO_2 during the Low-Pressure Arc-Discharge Plasma Synthesis

A. V. Ushakov[a, c], I. V. Karpov[a, c], A. A. Lepeshev[a, c]
[a] Siberian Federal University, Krasnoyarsk, 660041 Russia
[b] Krasnoyarsk Scientific Center, Siberian Branch, Russian Academy of Sciences, Krasnoyarsk, 660036 Russia
[c] Reshetnev Siberian State Aerospace University, Krasnoyarsk, 660014 Russia
e-mail: sfu-unesco@mail.ru

Abstract. The synthesis of titanium dioxide (TiO_2) nanoparticles with different percentage of anatase and rutile phases is investigated. The synthesis is performed by controlling the oxygen percentage in the gas mixture in the plasmachemical evaporation–condensation process employing a low-pressure arc discharge. In all our experiments, the pressure in the plasmachemical reactor and the average size of particles remain constant and are 60 Pa and 6 nm, respectively. The crystal structure of synthesized TiO_2 is studied using X-ray diffraction; the morphology of the particles is analyzed employing transmission electron microscopy. Using X-ray phase analysis, it is established that the concentration of the TiO_2 anatase phase decreases upon a decrease in the oxygen concentration in the gas mixture. It is shown that the TiO_2 anatase phase is more efficient for photocatalytic decomposition of methylene blue than the rutile phase.

Introduction

Titanium dioxide (TiO_2) is one of the most studied materials; it has many applications in industry and research, especially in photocatalysis [1, 2]. A comprehensive review of the surface properties of TiO_2, in which the interrelation between the structure and properties is emphasized, is given in [3]. The photoactivity of TiO_2 is pointed out in [4] as one of the most interesting and attractive properties. Experimental and theoretical investigations of the structural and electronic properties of TiO2 are described in [5]. TiO_2 can exist in a few stable crystalline forms the most widespread of which are anatase, rutile, and brookite [6]. The energy properties of TiO_2 polymorphs (relative to the rutile phase) was studied in [7], where it was found that they are lower by 0.71 kJ/mol for the brookite and are higher by 2.61 kJ/mol for the anatase. The brookite phase is stable only at very low temperatures and, therefore, is almost of no practical importance. The rutile and anatase phases usually coexist as mixed phases; that is why some efforts are necessary for obtaining the required pure phase. In recent years, the anatase phase of TiO_2 has aroused great interest owing to the technological applications in paints, pigments, and photocatalysis. It was reported that anatase has a higher photocatalytic activity than rutile [8]. Thus, the synthesis of TiO_2 with a preset crystalline phase on a large scale is of great practical importance. Although the chemical methods make it possible to obtain TiO_2 in large amounts [9], their structure, however, is mainly amorphous. It is shown in [10] that the presence of amorphous structure in TiO_2 reduces its photacatalytic activity and, consequently, the synthesis of nanocrystalline TiO_2 is an urgent problem. The results of chemical synthesis show that the time and the temperature of calcination greatly affect the TiO_2 nanopowder [11]. Although the phase transformations of TiO_2 during annealing of chemically synthesized TiO_2 have been studied by many researchers [12], the data on the temperatures in the reactions are controversial. Thus, the problem of controlling the crystal phase during the growth of a crystal from nanoparticles remains complicated for any chemical method as regards large-scale manufacturing. Nanocrystalline particles with an average size of smaller than 10 nm demonstrate higher photocatalytic properties than large-sized particles [13]. Thus, a detailed studying of the TiO_2 nanoparticles is also an important trend of investigation. It was shown in [14] that thermal processes in plasma are very efficient in the production of nanocrystalline materials on account their high temperature, high enthalpy, and high rate of hardening, which leads to homogeneous condensation of the gas phase. The reactor with a thermal rf plasma for the synthesis of pure

rutile and anatase TiO_2 nanoparticles by oxidizing of titanium nitride powder were employed in [15]. However, this method requires the raw material of coarse-grained TiH_2 powder, thus complicating the process.

Operating characteristics of a vacuum plasmachemical reactor for TiO_2 synthesis:

- Basic pressure in chamber – 10^{-3} Pa
- Arc discharge current – 100 A
- Voltage – 70 V
- Power – 10 kW
- Cooling water supply:
  (a) cathode – 1 L/min
  (b) substrate – 1 L/min
  (c) chamber walls – 2 L/min
- Plasma-forming gas (argon) supply – 60 Pa
- Reaction gas (oxygen) supply – 5, 10, 15, 20 vol % O_2

Thus, taking into account the growing need in the TiO_2 nanopowders, we employed the method of condensation from the gas phase for the synthesis of TiO_2 with the required crystalline phase. It is shown that the concentrations of anatase and rutile phases in synthesized TiO2 can be controlled by choosing an appropriate oxygen concentration inside the chamber.

Experimental

The morphological composition of the samples was analyzed on JEOL JEM-2100 transmission electron microscope. The samples for the electron microscopy study were prepared as follows: the powder was placed in isopropyl alcohol, dispersed in an ultrasonic bath for 2 min, and a solution drop was then placed on a carbon film substrate located on an electron-microscope support grid. The carbon film substrate was 10–15 nm thick. The phase composition of the obtained samples was investigated using the Advance D8 X-ray diffractometer in monochromated CuKα radiation. The scanning was carried out at room temperature in the angular range 30°–120° in 2θ with a step of 0.04°. The specific surface was measured by the BET method.

The spectra of the discharge plasma were measured using a flexible optical fiber with a diameter of 0.5 mm arranged near the evaporator cathode. The working section of the fiber was placed in a metal collimator with a diameter of 1.5 mm, to which negative potential (–300 V) relative to the vacuum chamber was supplied; the collimator shielded the fiber from the contact with the plasma and from the dusting by the cathode material. The remaining part of the fiber was closed by an opaque polyethylene tube. Radiation of the arc discharge plasma was registered by AvaSpec-2048USB2 spectrometer. This spectrometer makes it possible to register radiation spectra in the range 237–792 nm with a resolution of 0.7 nm.

The photocatalytic properties of the obtained nanoparticles of TiO_2 were analyzed by recording the photoabsorption peak (at 640 nm) of the aqueous solution of organic basic thiazine dye (methylene blue, MB) with an initial concentration of 100 mg/L after adding the TiO_2 synthesized powder and irradiating with ultraviolet radiation of the known duration. The absorption level was optimized for 7.2 mg of TiO_2 in the buffer solution.

Oxidation of Ti with TiO_2 formation is a highly exothermic reaction. The enthalpy of TiO_2 formation is –944.74 kJ/mol; therefore, the synthesis with the aid of the low-pressure plasmachemical process is very efficient. The experimental setup and the dependence of the powder properties on the conditions of sputtering were considered in detail in [16, 17]. The cathode made of VT1-00 titanium alloy with a diameter of 80 mm and a length of 100 mm was placed on a watercooled copper current distributor. An additional electrode was used for triggering a pilot arc, which made it possible to stabilize the plasma jet. The reactor chamber had a diameter of 0.60 m and a height of 0.60 m and was closed on both ends by flanges made of stainless steel with double walls. The chamber had two ports, one port for examining the arc

column during the metal evaporation and the other port for spectroscopic measurements of optical radiation.

The plasma-forming gas (argon) was supplied through the evaporator and produced a pressure of 60 Pa in the chamber. The evaporator power was 10 kW and the arc discharge direct current was 100 A; oxygen was used as the reaction gas with a flow rate maintained at a level of 5, 10, 15, and 20 vol % of the argon supply flow rate. Oxygen was supplied to the reactor in such a way that a homogeneous shell could be formed around the plasma flame. The reactor was preliminarily evacuated to a basic pressure of 10^{-3} Pa. The reaction products were collected during 10 min on a water-cooled hemispherical collector made of stainless steel and located at a distance of 0.12 m from the cathode. The table describes the operating parameters of the reactor during synthesis.

Results and discussion

The rate of TiO_2 synthesis was measured for various concentrations of oxygen. The output of the vacuum plasmachemical reactor was determined by measuring the loss of the mass of the cathode material and then, by measuring the weight of the collected nanoparticles synthesized for various concentrations of oxygen. For 5, 10, 15, and 20 vol % of O_2, the concentrations amounted to 15, 14.3, 12.1, and 11 g/h. The results show that the rate of production of synthesized TiO_2 decreases with an increase in the concentration of O_2. The efficiency of precipitation of the obtained material on the substrate was about 20 wt % relative to the total amount of the nanoparticles. The synthesized nanoparticles precipitated mainly on the reactor walls. For further studying, we used the nanoparticles collected on the substrate.

The X-ray diffraction pattern for the values of 2θ in the range from 22° to 30° is shown in Fig. 1. The most intense lines are determined from the JCPDS data as corresponding to the TiO_2 anatase (101) plane for 2θ = 25.3°, while an analogous peak appearing from the TiO_2 rutile (110) plane corresponds to 2θ = 27.4°. Relative concentrations of two crystalline phases were estimated using the intensities of the two lines mentioned above. The amplitudes of two peaks are shown together for four samples synthesized for 5, 10, 15, and 20 vol % of O_2. It should be noted that for these samples, relative intensities monotonically change. The amplitude of the anatase peak decreases upon a decrease in the concentration of O_2, while the rutile peak amplitude shows the inverse tendency. The ratio of the intensities of both phases is shown in Fig. 2.

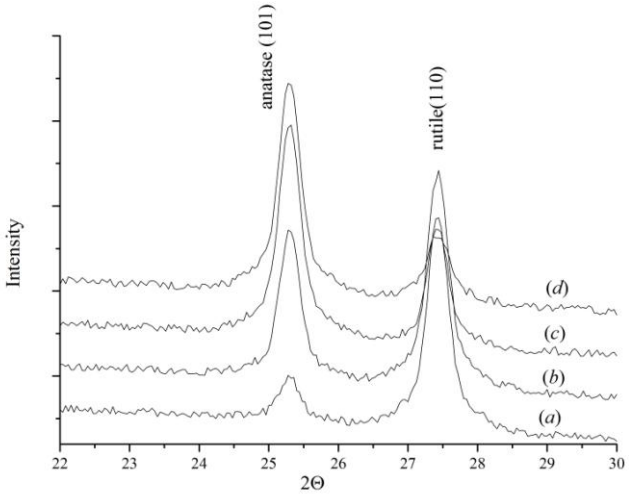

Fig. 1. X-ray diffraction pattern for the principal peak of the anatase (2θ = 25.30°, d = 3.52, hkl: (101)) and rutile (2θ = 27.43°, d = 3.25, hkl: (110)) phases of TiO_2 nanoparticles for (a) 5, (b) 10, (c) 15, and (d) 20 vol % of O_2.

A stable growth of the anatase phase from 0.3 to 2.4 means that the concentrations of O_2 during the synthesis strongly affect the formation of crystalline phases. It can also be seen from

Fig. 2 that the high concentration of O_2 facilitates the formation of anatase, while a reduction in the O_2 concentration facilitates the growth of the rutile phase. Changes in the crystalline phase upon variation of the O_2 concentration in the reactor can be connected with cluster chemistry of the vapor phase of the condensation. The presence of Ti–O clusters is confirmed by emission spectrum, whose typical region is shown in Fig. 3. The spectrum exhibits the fine structure of the Ti–O bands with the lines appearing at 665.1, 668.1, 671.9, 685.2, 705.4, 712.5, 719.7, and 726.9 nm. The wavelengths were compared with the values of the emission lines in [18]. These spectral lines indicate the presence of the Ti–O clusters in the arc plasma. These clusters subsequently diffuse from the hot plasma and then combine to form the crystallization centers in the immediate vicinity of the plasma flame boundaries. Obviously, the crystal phase of the nuclei is determined by two factors: (i) availability of oxygen for growth and (ii) the degree of supercooling during their formation. Accordingly, the concentration of oxygen directly influences the formation of the crystalline phases. As shown in [15], a low concentration of oxygen obtained by controlling the oxygen flow in the high-frequency thermal plasma reactor facilitates the growth of the rutile phase during the synthesis of TiO_2 from titanium nitride. Characteristic Raman bands of the TiO_2 rutile were detected at 147, 236, 447, and 611 cm^{-1} in the powders synthesized at low oxygen flow rates.

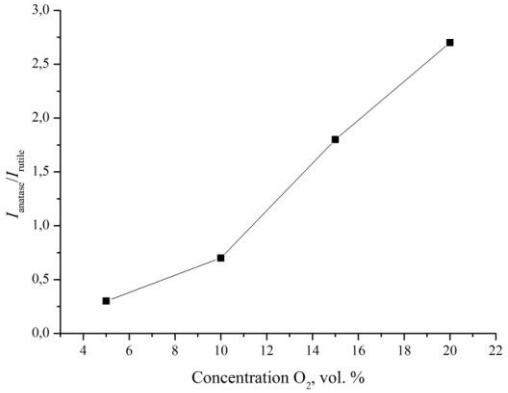

Fig. 2. Ratio of the intensities of the peaks of the principal lines of the anatase and rutile phases determined from the corresponding X-ray patterns (Fig. 1) as a function the O_2 concentration.

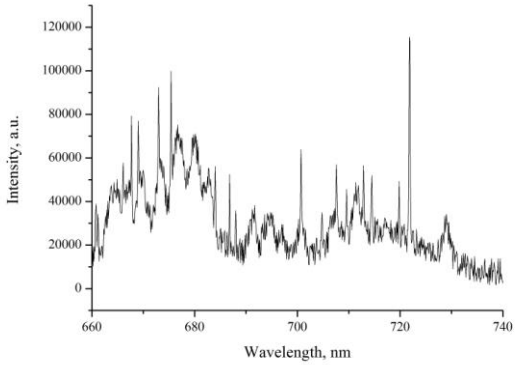

Fig. 3. Optical emission spectrum of the plasma during the TiO_2 synthesis.

The rate of cooling plays an important role in the crystallization process during the condensation of nanoparticles from the gas phase. Since the nanoparticles are synthesized under low pressure, the condensation conditions are far from thermodynamic equilibrium. High temperature gradients cause the formation of defect crystalline structures, a developed surface of the nanoparticles, oxygenation, and amorphization of the surface structures. A typical

micrograph of the sample is shown in Fig. 4a. The powder is an ensemble of strongly agglomerated particles of irregular shape with a size of 4 to 9 nm. Formations of up to 15 nm in size also detected; however, these agglomerates apparently consist of smaller particles. Such agglomerates cannot be disaggregated. As a rule, the particle shape is close to spherical. Analysis of the granulometric composition of the prepared nanoparticles has shown that the obtained nanopowder has a lognormal distribution, and the average particle size is 6 nm. The deviation from the average size does not exceed 40%.

To get information on the nanoparticle crystallinity, we analyzed the diffraction of electrons in the chosen region (Fig. 4b). The diffraction pattern clearly shows the spots, as well as diffused rings, which characterize the crystallinity of nanomaterials. The Miller indices in the diffraction pattern correspond to the TiO_2 anatase and rutile phases. It is quite obvious that the nanoparticles are crystalline, and this is in a good agreement with the results obtained by the X-ray fluorescence analysis. The micrographs obtained by the transmission electron microscopy (TEM) and the diffraction pattern do not differ significantly for four samples and, hence, from the micrograph shown in Fig. 4. The value of the specific surface calculated from the isotherm of low-temperature adsorption of argon is 446 m^2/g. If we use the well-known relation between surface area S, bottle density $\rho = 4$ g/cm^3, and average size of the particles $d = 6/\rho S$, we obtain 5 nm, which approximately corresponds to the TEM data.

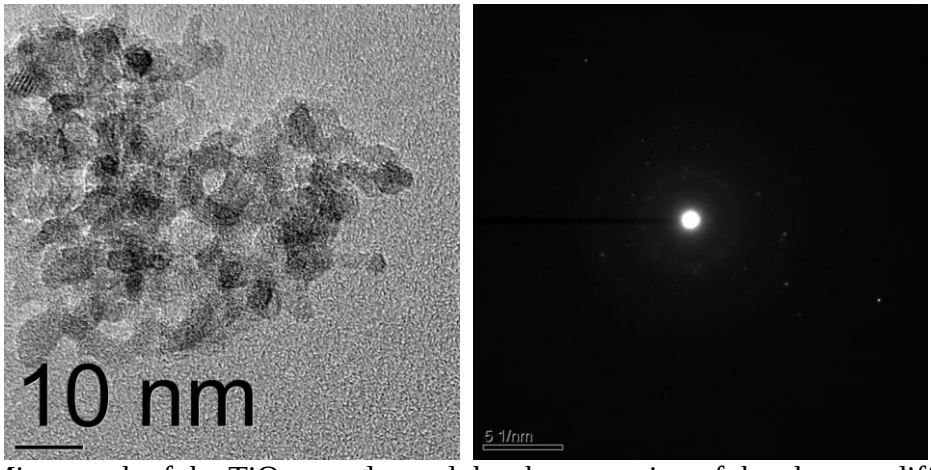

Fig. 4. Micrograph of the TiO_2 samples and the chosen region of the electron diffraction. The synthesis condition: the pressure of Ar in the plasmachemical reactor is 60 Pa and the O_2 concentration is 10 vol %.

The absorption spectra of methylene blue (MB) with TiO_2 synthesized for various concentrations of O_2 after ultraviolet irradiation during 150 min are shown in Fig. 5. It follows from the curves that photocatalytic properties of the obtained nanopowder increase with the concentration of O_2. The absorption level is reduced by 75%. Thus, the TiO_2 anatase phase has significantly better photocatalytic properties than the rutile phase.

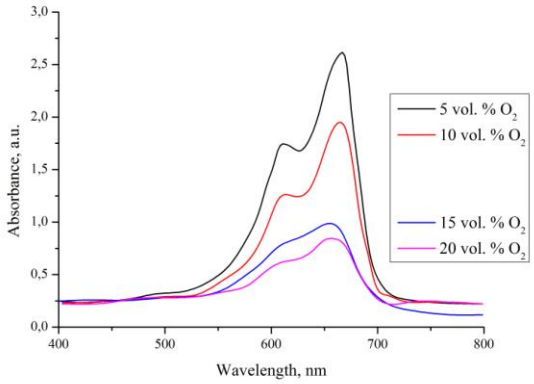

Fig. 5. Spectral characteristics of methylene blue with admixture of the TiO_2 nanoparticles synthesized for various concentrations of O_2 after ultraviolet irradiation during 150 min.

Conclusions

Thus, we have studied the influence of the oxygen concentration in a gas mixture on the ratio of the TiO_2 crystalline phases. High concentration of O_2 facilitates the formation of anatase, while a decrease in the concentration of O_2 stimulates the growth of the rutile phase. A change in the crystalline phase associated with the change in O_2 concentration in the reactor is connected with the cluster chemistry of the vapor phase of condensation. The Ti–O clusters diffuse from the hot plasma and then combine to form crystallization centers near the boundaries of the plasma flame. In accordance with the oxygen concentration, one or the other phase of TiO_2 is formed. The anatase phase of TiO_2 has significantly better photocatalytic properties than the rutile phase.

Acknowledgments

This study was financially supported by the Russian Foundation for Basic Research (project no. 15-08-02132) in the framework of the program "Investigation of Vacuum Plasma-Chemical Processes of Evaporation and Condensation of a Material in Vapor–Plasma Flows with Subsequent Formation of Nanoparticles with Unique Physicochemical Properties."

References

1. M. Schiavello, Photocatalysis and Environment Trends and Applications, NATO ASI Ser. (Kluwer Academic, Dordrecht, 1988).

2. D. F. Ollis and H. Al-Ekabi, Photocatalytic Purification and Treatment of Water and Air (Elsevier, Amsterdam, 1993).

3. U. Diebold, Surf. Sci. Rep. 48, 53 (2003).

4. A. Fujishima and K. Honda, Nature 238, 37 (1972).

5. U. Diebold, Surf. Sci. Rep. 48, 53 (2003).

6. G. V. Samsonov, The Oxide Handbook (IFI/Plenum, New York, 1982).

7. M. R. Ranade, A. Navrotsky, H. Z. Zhang, J. F. Banfield, S. H. Elder, A. Zaban, P. H. Borse, S. K. Kulkarni, G. S. Doran, and H. J. Whitfield, Proc. Natl. Acad. Sci. USA 99, 6476 (2002).

8. X. F. Zhou, D. B. Chu, S. W. Wang, C. J. Lin, and Z. Q. Tian, Mater. Res. Bull. 37, 1851 (2002).

9. B. Li, X. Wang, M. Yan, and L. Li, Mater. Chem. Phys. (2002).

10. L. Gao and Q. Zhang, Scr. Mater. 44, 1195 (2001).

11. B. Li, X. Wang, M. Yan, and L. Li, Mater. Chem. Phys. 78, 184 (2002).

12. E. Haro-Poniatowski, R. Rodri'guez-Talavera, M. de la Cruz Heredia, O. Cano-Corona, and R. Arroyo-Murillo, J. Mater. Res. 9, 2102 (2102).

13. L. Gao and Q. Zhang, Sci. Mater. 44, 1195 (2001).

14. I. V. Karpov, A. V. Ushakov, L. Yu. Fedorov, and A. A. Lepeshev, Tech. Phys. 59, 559 (2014).
15. S. Oh and T. Ishigaki, Thin Solid Films 457, 186 (2004).
16. A. V. Ushakov, I. V. Karpov, and A. A. Lepeshev, Materialovedenie, No. 3, 48 (2012).
17. A. V. Ushakov, I. V. Karpov, A. A. Lepeshev, et al., Remont Vosstanovlenie, Modernizatsiya, No. 9, 41 (2012).
18. A. N. Zaidel, V. K. Prokofev, S. M. Raiskii, V. A. Slavnyi, and E. Ya. Shreider, Tables of Spectral Lines (Plenum, New York, 1970).